

# Wormlike Micelle Assisted Rod Coating: A General Method for Facile Fabrication of Large-Area Conductive Nanomaterial Thin Layer onto Flexible Plastics

Jingyi Xie, Huan Wang, Huadong Bai, Peng Yang, Mengxue Shi, Peng Guo, Chen Wang, Wantai Yang,\* and Huaihe Song

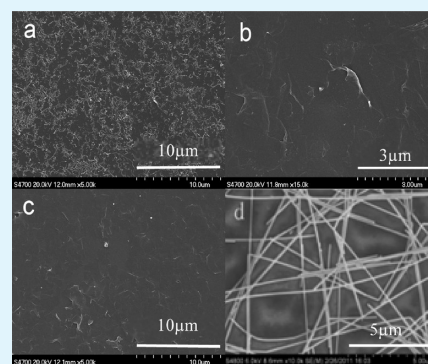
State Key Laboratory of Chemical Resource Engineering, Beijing 100029, China

College of Materials Science and Engineering, Beijing University of Chemical Technology, Beijing 100029, China

## Supporting Information

**ABSTRACT:** Through combined application of wormlike-micelle and rod-coating technique, a general method was demonstrated for the facile preparation of thin transparent conductive films (TCF) of various nanomaterials and their hybrids on flexible plastics. The cetyltrimethylammonium hydroxide (CTAOH)/p-toluenesulfonic acid (CTAT) wormlike micelle system was selected for both the dispersion of different nanomaterials and the enhancement of viscosities of the coating fluids. With the single-walled carbon nanotubes (SWNTs)/wormlike micelle aqueous dispersions as coating fluid, TCFs of SWNTs on flexible poly(ethylene terephthalate) (PET) substrates made by rod-coating method were demonstrated. After doping by immersion into thionyl chloride solution, the sheet resistance of SWNTs thin films, which had a transmittance of about 78%, was as low as 480 $\Omega$ /sq. This coating method was extended to the preparation of thin films or networks of other materials such as reduced graphene oxide and Ag nanowires. The obtained TCF from Ag nanowire networks has a low sheet resistance of 17 $\Omega$ /sq, which is comparable to the value of best indium tin oxide (ITO) coating on plastic substrates. Finally, hybrid thin films of different nanomaterials were demonstrated by this method.

**KEYWORDS:** wormlike micelle, rod coating, transparent, large-area conductive layer, flexible, hybrid film



## INTRODUCTION

Thin, transparent, conductive films (TCFs) serve as crucial components in various electronic devices, including head up displays, organic light emitting diodes, and plastic solar cells.<sup>1–3</sup> Although tin-doped indium oxide (ITO) thin films have been widely utilized as transparent electrodes for decades, the brittleness as well as the high price of ITO inhibits their further applications in the area of flexible electronics.<sup>4</sup> Fortunately, the rapid development of nanotechnology provides various alternative materials such as single-walled carbon nanotubes (SWNTs), graphene sheets, and metal nanowires for the replacement of ITO. To fabricate TCFs based on these novel nanomaterials, researchers have developed solution-based methods<sup>5–9</sup> such as filtration,<sup>10–15</sup> spin coating,<sup>16–23</sup> and spray coating.<sup>24,25</sup> These methods offer several advantages such as low processing temperatures and the avoidance of expensive equipment.<sup>26</sup> However, because of the size limitation of the filter and the inhomogeneity of carbon nanotube films caused by the spin coating or spray coating,<sup>16,3,26</sup> great challenges still exist for large-scale processing of these materials if they are to result in transparent, homogeneous thin films.

The rod coating method, in which the precoated substrate passes under a wire-wrapped cylinder to meter off excess coating, has long been considered as a continuous and scalable approach to fabricate thin films of various materials in industry,

and has recently emerged as a promising method for large scale fabrication of transparent conducting thin films of nanomaterials. Dan et al. first reported a rod coating approach for the continuous and scalable fabrication of transparent SWNTs films.<sup>27</sup> In their work, a SWNTs-SDBS-Triton 100 aqueous solution was chosen as the coating fluid, and large area SWNTs thin film were obtained. Recently, a scalable rod coating method for the preparation of Ag nanowires networks was also developed<sup>28</sup> by Hu et al. via the use of methanol as a nonaqueous organic solvent. Despite these promising results, to our best knowledge, the fabrication of TCFs based on graphene or reduced graphene oxides (RGO), as well as hybrid materials which combine unique properties together from individual components, are unexplored until now. The latter is especially important since it has been recently found that hybrid thin films are of great merit in device applications.<sup>29</sup> For this aim, a general dispersion system which is compatible with various nanomaterials has to be applied, so that the mixing of the coating fluid based on different nanomaterials could become effective for the fabrication of TCFs. From this point of view, the reported approaches based on SDBS-Triton 100 aqueous

Received: December 22, 2011

Accepted: May 3, 2012

Published: May 3, 2012

solution and methanol are not desirable, due to great differences between dispersion systems used in these two methods.

To address the above problems, we pay attention to the wormlike micelle-based dispersion system. During the past two decades, wormlike micelle systems which show interesting viscoelastic properties have been widely investigated<sup>30–34</sup> and exploited to obtain well-dispersed SWNTs solutions.<sup>35–37</sup> Enlightened by these works, we have fabricated transparent conductive thin films and networks with the assistance of wormlike micelles. Wormlike micelles are chosen as the coating fluid for the following reasons: (1) the rheology properties of wormlike micelles are sensitive to temperature and the ratio between cationic and anionic ions, so that the viscosity of the coating fluid is conveniently adjustable.<sup>30–34,38</sup> (2) The viscosity of the wormlike micelle system is induced by the self-assembly of ionic surfactants and the presence of other nanostructures,<sup>39–41</sup> which often increase the viscosity of such systems. The wormlike micelle based coating fluid technique could be extended to various nanostructures including SWNTs, multiwalled-carbon nanotubes (MWNTs), graphene, or metal nanomaterials. (3) Various wormlike micelle systems with different surfactants are available for the preparation of nanomaterial thin films,<sup>34,38,44</sup> so the design flexibility is greatly enhanced. (4) Unlike polymer-based dispersion systems, surfactants and organic counterions in the wormlike micelles can be easily removed from dried SWNTs/surfactant composite thin films, in order to prepare SWNTs based transparent thin films.<sup>30</sup> In the present work, we proposed for the first time that the combination of wormlike micelle dispersion systems and rod-coating techniques could afford a general dispersion and coating method for the fabrication of TCFs from various nanomaterials and their hybrids on flexible plastics.

In this manuscript, we first selected SWNTs as a model material with which to demonstrate our strategy design, and then the wormlike micelle assisted rod coating method was extended to the preparation of thin films based on other nanomaterials such as reduced graphene oxide (RGO) and Ag nanowires. Finally, a one-step method for the fabrication of hybrid films of different nanomaterials was demonstrated with this strategy.

## EXPERIMENTAL SECTION

**Materials.** Both the SWNTs (purity 90%, diameter <2 nm) and the MWNTs (purity 95%, diameter 10–20 nm) were purchased from Chengdu Organic Chemicals Co. Ltd. and were synthesized by chemical vapor deposition. SWNTs were further purified by reflux in 7 M HNO<sub>3</sub> for 3 h. Cetyltrimethylammonium hydroxide (CTAOH) was purchased from Tokyo Chemical Industry Co. Ltd. *p*-toluenesulfonic acid was purchased from Beijing Chemical Reagent Corp. AgNO<sub>3</sub> and ethylene glycol were purchased from Beijing Chemical Works. Artificial graphite was provided by Dong Xin Electrical Carbon Co. Ltd., with a nominal size of 15 μm. Graphene oxides were synthesized through the modified Staudenmaier's method reported in our previous work.<sup>41</sup> Ag nanowires were purchased from Blue Nano, Inc.

**Preparation of SWNTs Fluid.** In a typical experiment, 15 mg of SWNTs were added into 15 mL of 0.05 M CTAOH/water solution, and then sonicated with ultrasonic cell disruption at 100W for 10 min. The resulting black suspension was centrifuged at 9000 rpm for 15 min. After the centrifugation, 10 mL of the supernatant suspension was carefully recovered. The viscoelasticity of the SWNTs suspension was adjusted by dropwise addition of 1 mL of 0.45 M *p*-toluenesulfonic acid aqueous solution into the SWNTs suspension.

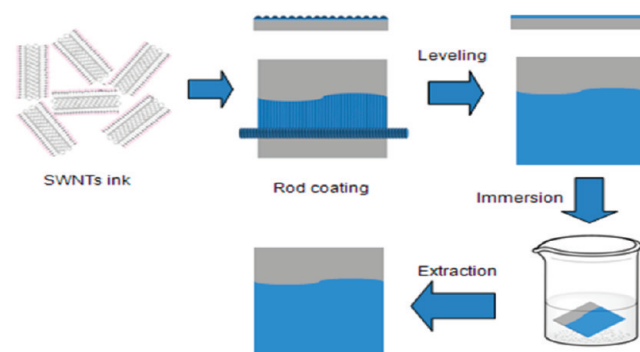
**Fabrication of SWNTs Thin Films.** Four-tenths of a milliliter of freshly prepared SWNTs fluid was poured onto a 50 μm thick polyethylene terephthalate (PET) substrate. Then, a Mayer rod was pulled over the fluid to form a uniform thin film of the SWNTs suspensions on the PET substrate at 50 °C. The wet SWNTs fluid was then dried at 20 °C, which produced a thin layer containing SWNTs and surfactants. The surfactants were further removed by immersing the SWNT film into ethanol solution for 24 h, followed by extraction with ethanol for 48 h.

**Characterization.** The morphology of the SWNTs transparent thin films was observed by a scanning electron microscope (SEM, Hitachi S-4700 operated at 20 kV) and atomic force spectroscopy (AFM, NanoscopeIII Digital Instruments/Veco Metrology Group). X-ray photoelectron spectra (XPS) of the samples were measured with an ESCALAB 250 (VG Scientific) photoelectron spectrometer using monochromatic Al KR radiation. The viscosity of the wormlike micelles was studied with controlled-stress Haake RS150 rheometer, using a C60/1 cone and plate sensor system. The viscosity of the CTAOH aqueous solution was measured by a DG 41 double gap sensor system. The sheet resistances of SWNTs transparent thin films were recorded on a SX1934 four-point testing instrument.

## RESULTS AND DISCUSSION

When applying the rod coating method to prepare a uniform thin layer, two criteria must be fulfilled. First, the spreading of the coating fluid through a Mayer rod must lead to a ribbed or waved surface (see the Supporting Information, Figure S1, and Scheme 1). Driven by the surface tension, the ribbed liquid

### Scheme 1. Schematic Illustration of the Procedure for Preparing SWNT-Based Transparent Thin Films through the Rod Coating Method



layer of coating fluid could gradually level to a homogeneous thin film (Scheme 1). However, the leveling process is resisted by the viscosity of the coating fluid.<sup>42</sup> The leveling time of the coating fluid is proportional to its viscosity, which means that the viscosity of the coating fluid has to be low enough to avoid the formation of a waved surface.<sup>43</sup> For the rod coating method, the optimum viscosity range of coating fluids is between 0.02 and 1 Pa S.<sup>44</sup> In addition, during the drying process, the dewetting process or gravitational force will induce secondary flow; to maintain the uniformity of the SWNTs film, the viscosity of the SWNTs fluid should be high enough to hinder the secondary flow caused by the dewetting after coating. Therefore, a good balance that controls the viscosity of the SWNTs fluid is critical for the fabrication of high-quality SWNTs films on substrates.

In this work, the well-studied CTAOH-*p*-toluenesulfonic acid–water (CTAT) wormlike micelle system was used for the preparation of SWNTs fluid. The *p*-toluenesulfonic groups insert into the headgroups of the micelles at a depth and induce

the elongation of micelles. Similar to polymeric systems, wormlike micelles or threadlike micelle systems show interesting rheological behaviors due to the entanglement between micelles.<sup>45–47,33</sup> Generally, the addition of nanoparticles into wormlike micelle systems will enhance the viscosity of the whole system, due to the formation of a so-called “double network”.<sup>48</sup> Because of the different surface chemistries of various nanoparticles, the interactions between wormlike micelles and nanoparticles range from electrostatic forces<sup>39,40,48</sup> to noncovalent wrapping,<sup>35</sup> which drive the dispersion of SWNTs in our system.

Figure 1 shows the viscosity of a CTAT wormlike micelle system at different temperatures. The mole ratio of CTAOH/*p*-

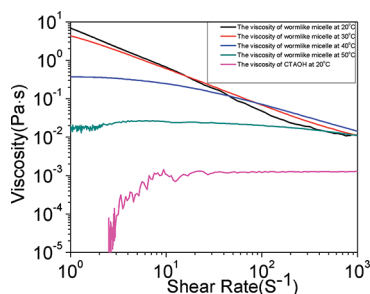


**Figure 1.** Viscosity vs shear rate for the CTAOH aqueous solution and CTAOH/*p*-toluenesulfonic acid wormlike micelle system at different temperatures.

toluenesulfonic acid is 10/9. Although the viscosity of CTAOH was at the order of  $1 \times 10^{-3}$  Pa s at 20 °C, the viscosity of the wormlike micelle system increased by 4 orders of magnitude at the same temperature, with the adding of *p*-toluenesulfonic acid into the CTAOH system. As the temperature increased, the viscosity of the wormlike micelle system decreased drastically. This phenomenon was possibly induced by the decreasing of the average length of wormlike micelles, caused by the higher thermal fluctuation induced by the elevation of temperatures.<sup>38,49–51</sup> Temperature also exhibited a strong influence on the shear-thinning property of the wormlike micelle system. The shear-thinning property was obvious at lower temperatures up to 40 °C, because of the scission of micelles at high shearing rates.<sup>52,53</sup> When the temperature was further increased to 50 °C, the wormlike micelles behaved almost like a Newtonian fluid.<sup>54</sup> Therefore, to satisfy these two requirements mentioned above simultaneously, the coating processes were performed on a hot stage with the temperature holding at 50 °C. At 50 °C, the viscosity of the wormlike micelle was equal to 0.02 Pa·s, and kept constant with the change of shearing rate. As mentioned above, the introduction of SWNTs brings an elevation of the system viscosity.<sup>39,55</sup> Nonetheless, the final viscosity of the SWNT-micelle system should be still in the optimum viscosity range (0.02–1 Pa s) for the coating fluid, because the viscosity increase resulting from the adding of SWNTs is usually confined with a range of 1 order of magnitude.<sup>55</sup> As a result, a homogeneous thin film of SWNTs was achieved by pulling the Mayer rod over the SWNTs fluid on the PET substrate. The coated film was then dried at 20 °C because the high zero shear viscosity of the wormlike micelle at 20 °C prevented the flow and dewetting during the drying of the SWNTs fluids.

Another criterion of SWNTs fluids relates to the stability of the SWNTs dispersion after mixing in other additives. It has been reported that the adding of salt or changing pH would

reduce the electrostatic repulsion between surfactant molecules, and decrease the interaction between the surfactant and SWNTs. Consequently, the SWNTs suspension solution is extremely sensitive toward additives, and any inappropriate additives could lead to the aggregation and coagulation of the SWNTs in the dispersion.<sup>56,57</sup> In our work, the SWNTs dispersion was stable for more than 24 h at room temperature when the mole ratio of CTAOH and *p*-toluenesulfonic acid was 10:9. At this ratio, all *p*-toluenesulfonic acid added into the CTAOH/SWNTs dispersion was neutralized by CTAOH. With the decrease in the mole ratio between CTAOH and *p*-toluenesulfonic acid, the extra *p*-toluenesulfonic acid cannot be neutralized by surfactant CTAOH, and the SWNTs in the dispersion aggregate immediately (see the Supporting Information, Figure S2).

A PET film with a large-area SWNTs coating, 25 cm × 10 cm, was further obtained by the wormlike micelle assisted rod coating method (Figure 2c), which showed good optical

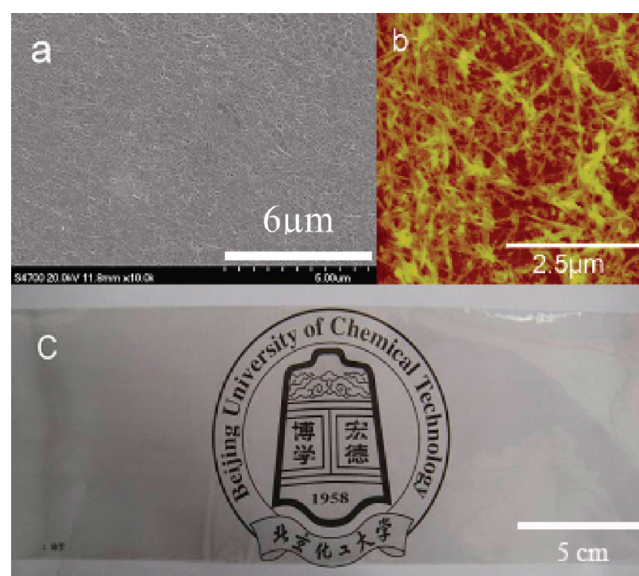


**Figure 2.** (a) SEM, (b) AFM, and (c) optical images of SWNT thin films on a PET substrate, prepared through the rod coating method with the assistance of wormlike micelles. In c, a 25 cm long PET substrate with SWNTs thin coating is shown as a transparent film.

transparency. The surface morphology of SWNTs thin films was investigated by both SEM (Figure 2a) and AFM measurements (Figure 2b). Homogeneous coatings consisting of interconnected nanotube networks were observed. The density distribution of SWNTs bundles was also investigated through counting the number of SWNTs bundles in 1 square micrometer at different sites. For an 80% transparency SWNTs thin film, mostly, the number of SWNTs bundles within 1 square micrometer is between 140 and 180, which further demonstrates the homogeneity of SWNTs in the thin layers (see the Supporting Information, Figure S3).

Because the residual surfactant trapped in the SWNTs transparent thin film will induce additional resistance, the removal of such surfactants after the rod-coating and drying process could greatly decrease the sheet resistance of the SWNTs transparent films. In this work, a multistep method is adopted for the removal of CTAT. Large amounts of surfactants introduced on the PET substrate were removed by a simple immersion process. The small amount of remaining

surfactants was further eliminated through extraction, which was reported as a highly efficient method for the removal of residual surfactants.<sup>11</sup> The atomic percentage of N for CTAOH and S for p-toluenesulfonic acid could serve as an effective indicator for the amount of residual surfactants. Figure 3 shows

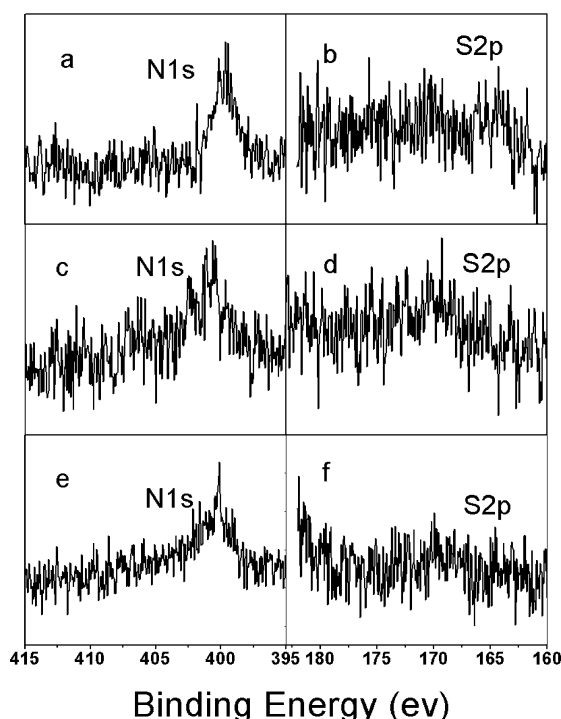


**Figure 3.** XPS measurement of PET films before and after coating with a thin layer of SWNTs. (a) N1s spectra on a pristine PET film; (b) S2p spectra on a pristine PET film; (c) N1s spectra on a PET film coated with a thin layer of SWNTs after immersion; (d) S2p spectra on a PET film coated with a thin layer of SWNTs after immersion; (e) N1s spectra on a PET film coated with a thin layer of SWNTs after extraction; (f) S2p spectra on a PET film coated with a thin layer of SWNTs after extraction.

XPS analysis of a pristine PET film, and the SWNTs coated PET film after immersion and solvent extraction. As shown in panels a and b in Figure 3, there are small amounts of N on the surface of the pristine PET substrate which may be attributed to additives. Also, the S2p spectrum indicates that no S is present on the surface of the PET substrate. After immersion, The N1s and S2p peaks demonstrate that the residual surfactant remained in the SWNTs thin layer (Figure 3c and 3d). Further extraction clearly removed p-toluenesulfonic groups absorbed in the SWNTs thin layer, because the S2p signal on the SWNT-coated film was measured at zero, as was the level on the pristine PET film (Figure 3f). However, the atomic percentage of N on SWNTs coated PET films after extraction is still 0.82% (Figure 3e), which can be ascribed to two sources, the N containing additives in the PET substrates, and the small amount of cationic surfactants adsorbed on the surface of the SWNTs because of the electrostatic force between the cationic surfactants and the carboxyl groups on the ends and sidewalls of carbon nanotubes.

For the purpose of reducing the sheet resistance of SWNTs based transparent thin films, several dopants including high-concentration HNO<sub>3</sub>, oleum, or thionyl chloride were utilized to dope the SWNTs thin film.<sup>11,27</sup> In this work, all SWNTs thin

films were immersed into thionyl chloride for 20 min, followed by rinsing with ethanol 3 times to decrease the resistance of SWNTs films. The sheet resistance versus transmittance curve for films with different thicknesses of SWNTs was shown in Figure 4. After the coating and removal of surfactants, a sheet

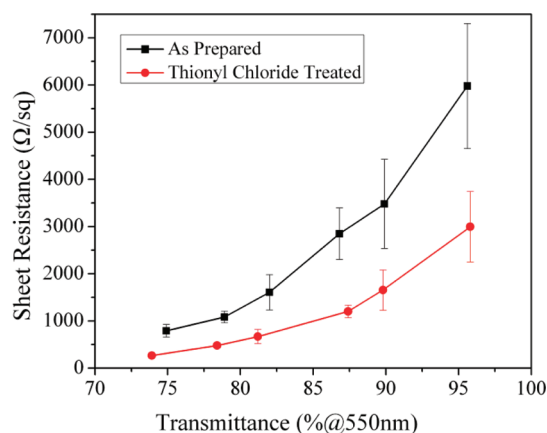


**Figure 4.** Sheet resistance versus transmittance for SWNT-based thin films before and after thionyl chloride treatment.

resistance of 1086 Ω/sq for corresponding transmittances of 78% was achieved. The sheet resistance could be further reduced to 480 Ω/sq by thionyl chloride treatment, without significant impact on the transmittance of the SWNTs film (see the Supporting Information, Figure S4).

An inherent advantage of using wormlike micelles is that such a system is particularly effective for the dispersion of various nanomaterials, and the adding of different nanostructures often enhances the viscosity of wormlike micelles systems.<sup>35,39–41,55</sup> Therefore, there is a great chance to extend this rod coating method conveniently to a variety of nanostructures. Figure 5 shows the SEM images of MWNTs, graphene oxide (GO), and Ag nanorod thin films on the PET substrate prepared by using this wormlike micelle dispersion as

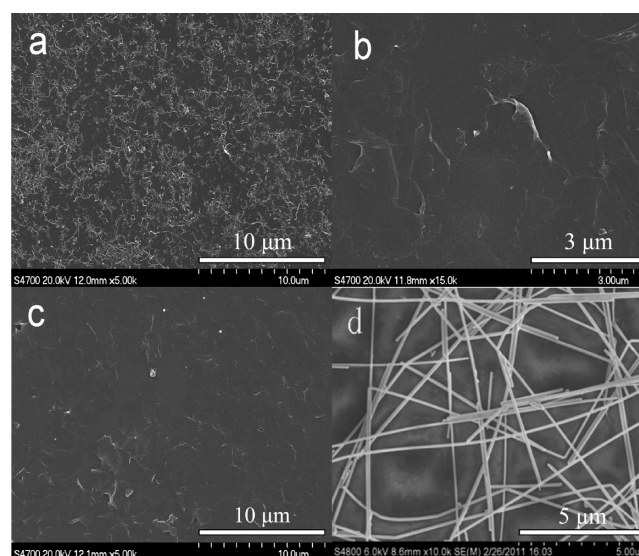


**Figure 5.** SEM images of various nanomaterial-based thin film prepared through the rod coating technique with wormlike micelle dispersions as the coating fluid: (A) MWNTs; (B) GO; (C) RGO; (D) Ag nanowire network.

the coating fluid. Similar to the case of SWNTs, a uniform thin layer of different nanostructures could be observed. The GO thin film coated on the PET substrate (Figure 5b) could be further reduced by simply immersing it into 1% hydrazine monohydrate solution at 90 °C for 12 h, which lead to a conductive, reduced GO (RGO) film (see the Supporting Information, Figures S5–S7). The sheet resistance of the Ag nanowire network is 17.3Ω/sq at a transmittance of 85% at 550 nm. In addition, hybrid thin films of different nanomaterials could also be prepared by this method (see the Supporting Information, Figures S8–S11).

## CONCLUSION

In summary, through the combination of the viscoelastic CTAT wormlike micelle system and the rod coating technique, a facile method for the fabrication of transparent high conductive film (TCFs) on flexible PET substrate was demonstrated in this work. Comparison with reported rod-coating techniques which only offer a single application, this method offers a general dispersion system for preparing coating fluids that could be applied to versatile conductive nanomaterials such as SWNTs, MWNTs, Ag nanowires, GO, and hybrid films made from them. The use of organic solvents to disperse the nanomaterials, especially Ag nanowires, is excluded to afford low-cost and environmentally benign compatibility. Given the wide application of the rod coating method for the scalable coating of different materials onto flexible substrates, the method developed in this manuscript shows great merit both for the industrialization of flexible electronic devices and the scalable deposition of various nanostructures onto different surfaces.

## ASSOCIATED CONTENT

### Supporting Information

UV–vis spectra data of SWNTs thin films, XPS data for the reduced graphene oxide film, SEM images and sheet resistance data of the reduced graphene oxide film, Ag nanowires networks and various hybrid films. This material is available free of charge via the Internet at <http://pubs.acs.org>.

## AUTHOR INFORMATION

### Corresponding Author

\*E-mail: yangwt@mail.buct.edu.cn. Fax: 86-10-64416338.

### Notes

The authors declare no competing financial interest.

## ACKNOWLEDGMENTS

We are thankful for the helpful discussion from Dr. Wangyang Fu, Dr. Bin Wu, and Dr. Liping Huang. Financial support for this study was provided by the Key Project of National Natural Science Foundation of China (Grant 51033001) and National High Technology Research and Development Program (863 Program 2009AA03Z325).

## REFERENCES

- (1) Gruner, G. J. *Mater. Chem.* **2006**, *16*, 3533–3539.
- (2) Gordon, R. G. *MRS Bull.* **2000**, *25*, 52–57.
- (3) Hu, L.; Hecht, D. S.; Gruner, G. *Chem. Rev.* **2010**, *110*, 5790–5844.
- (4) Kumar, A.; Zhou, C. W. *ACS Nano* **2010**, *4*, 11–14.
- (5) Neerja, S.; Parikh, K.; Suh, D. S.; Munoz, E.; Kolla, H.; Manohar, S. K. *J. Am. Chem. Soc.* **2004**, *126*, 4462–4463.
- (6) Andrade, M. J. D.; Lima, M. D.; Skákalová, V.; Bergmann, C. P.; Roth, S. *Phys. Status Solidi RRL* **2007**, *1*, 178–180.

- (7) Lee, J. Y.; Connor, S. T.; Cui, Y.; Peumans, P. *Nano Lett.* **2008**, *8*, 689–692.
- (8) Wang, X.; Zhi, L. J.; Müllen, K. *Nano Lett.* **2008**, *8*, 323–327.
- (9) Vichchulada, P.; Zhang, Q.; Duncan, A.; Lay, M. D. *ACS Appl. Mater. Interfaces* **2010**, *2*, 467–473.
- (10) Wu, Z. C.; Chen, Z. H.; Du, X.; Logan, J. M.; Sippel, J.; Nikolou, M.; Kamaras, K.; Reynolds, J. R.; Tanner, D. B.; Hebard, A. F.; Rinzler, A. G. *Science* **2004**, *305*, 1273–1276.
- (11) Wang, Y.; Di, C. A.; Liu, Y. Q.; Kajitara, H.; Ye, S.; Cao, L.; Wei, D.; Zhang, H.; Li, Y.; Noda, K. *Adv. Mater.* **2008**, *20*, 4442–4449.
- (12) Zhou, Y. X.; Hu, L. B.; Gruner, G. *Appl. Phys. Lett.* **2006**, *88*, 123109.
- (13) Zhang, D.; Ryu, K.; Liu, X.; Polikarpov, E.; Ly, J.; Tompson, M. E.; Zhou, C. *Nano Lett.* **2006**, *6*, 1880–1886.
- (14) De, S.; Higgins, T. M.; Lyons, P. E.; Doherty, E. M.; Nirmalraj, P. N.; Blau, W. J.; Boland, J. J.; Coleman, J. N. *ACS Nano* **2009**, *3*, 1767–1774.
- (15) Eda, G.; Fanchini, G.; Chhowalla, M. *Nat. Nanotechnol.* **2008**, *3*, 270–274.
- (16) Hellstrom, S. L.; Lee, H. W.; Bao, Z. N. *ACS Nano* **2009**, *3*, 1423–1430.
- (17) LeMieux, M. C.; Sok, S.; Roberts, M. E.; Opatkiewicz, J. P.; Liu, D.; Barman, S. N.; Patil, N.; Mitra, S.; Bao, Z. *ACS Nano* **2009**, *3*, 4089–4097.
- (18) Williams, Q. L.; Liu, X.; Walters, W.; Zhou, J. G.; Edwards, T. Y.; Smith, F. L.; Williams, G. E.; Mosley, B. L. *Appl. Phys. Lett.* **2007**, *91*, 143116.
- (19) Jo, J. W.; Jung, J. W.; Lee, J. U.; Jo, W. H. *ACS Nano* **2010**, *4*, 5382–5388.
- (20) Chang, H. X.; Wang, G. F.; Yang, A.; Tao, X.; Liu, X.; Shen, Y.; Zheng, Z. *Adv. Funct. Mater.* **2010**, *20*, 2893–2902.
- (21) Wu, J. B.; Becerril, H. A.; Bao, Z. N.; Liu, Z. F.; Chen, Y.; Peumans, P. *Appl. Phys. Lett.* **2008**, *92*, 263302.
- (22) Becerril, H. A.; Mao, J.; Liu, Z. F.; Stoltenberg, R. M.; Bao, Z.; Chen, Y. *ACS Nano* **2008**, *2*, 463–470.
- (23) Wu, J. B.; Agrawal, M.; Becerril, H. A.; Bao, Z.; Liu, Z.; Chen, Y.; Peumans, P. *ACS Nano* **2010**, *4*, 43–48.
- (24) Geng, H. Z.; Kim, K. K.; So, K. P.; Lee, Y. S.; Chang, Y.; Lee, Y. H. *J. Am. Chem. Soc.* **2007**, *129*, 7758–7759.
- (25) Kaempgen, M.; Duesberg, G. S.; Roth, S. *Appl. Surf. Sci.* **2005**, *252*, 425–429.
- (26) Lu, F. S.; Mezziani, M. J.; Cao, L.; Sun, Y. P. *Langmuir* **2011**, *27*, 4339–4350.
- (27) Dan, B.; Irvin, G. C.; Pasquali, M. *ACS Nano* **2009**, *3*, 835–843.
- (28) Hu, L. B.; Kim, H. S.; Lee, J. Y.; Peumans, P.; Cui, Y. *ACS Nano* **2010**, *4*, 2955–2963.
- (29) Tung, V. C.; Huang, J. H.; Tevis, I.; Kim, F.; Kim, J.; Chu, C. W.; Stupp, S. I.; Huang, J. *J. Am. Chem. Soc.* **2011**, *133*, 4940–4947.
- (30) Yang, J. *Curr. Opin. Colloid Interface Sci.* **2002**, *7*, 276–281.
- (31) Herrington, K. L.; Kaler, E. W.; Miller, D. D.; Zasadzinski, J. A.; Chiruvolu, S. *J. Phys. Chem.* **1993**, *97*, 13792–13802.
- (32) Lin, Z.; Cai, J. J.; Scriven, L. E.; Davis, H. T. *J. Phys. Chem.* **1994**, *98*, 5984–5993.
- (33) Koehler, R. D.; Raghavan, S. R.; Kaler, E. W. *J. Phys. Chem. B* **2000**, *104*, 11035–11044.
- (34) Raghavan, S. R.; Fritz, G.; Kaler, E. W. *Langmuir* **2002**, *18*, 3797–3803.
- (35) Kim, T. H.; Doe, C. W.; Kline, S. R.; Choi, S. M. *Adv. Mater.* **2007**, *19*, 929–933.
- (36) Kim, T. H.; Doe, C. W.; Kline, S. R.; Choi, S. M. *Macromolecules* **2008**, *41*, 3261–3266.
- (37) Doe, C. W.; Jang, H. S.; Kline, S. R.; Choi, S. M. *Macromolecules* **2010**, *43*, 5411–5416.
- (38) Han, Y.; Feng, Y.; Sun, H.; Li, Z.; Han, Y.; Wang, H. *J. Phys. Chem. B* **2011**, *115*, 6893–6902.
- (39) Helgeson, M. E.; Hodgdon, T. K.; Kaler, E. W.; Wagner, N. J. *Langmuir* **2010**, *26*, 8049–8060.
- (40) Bandyopadhyay, R.; Sood, A. K. *J. Colloid Interface Sci.* **2005**, *283*, 585–591.

- (41) Guo, P.; Song, H.; Chen, X. *J. Mater. Chem.* **2010**, *20*, 4867–4874.
- (42) Tracton, A. A. *Coating Technology Handbook*. 3rd ed.; CRC Press: Boca Raton, FL, 2006.
- (43) Koleske, J. V. *Paint and Coating Testing Manual: Fourteenth Edition of the Gardner-Sward Handbook*; ASTM: Philadelphia, 1995.
- (44) Cohen, E.; Gutoff, E. *Modern Coating and Drying Technology*; VCH: New York, 1992.
- (45) Truong, M. T.; Walker, L. M. *Langmuir* **2000**, *16*, 7991–7998.
- (46) Schubert, B. A.; Kaler, E. W.; Wagner, N. J. *Langmuir* **2003**, *19*, 4079–4089.
- (47) Kaler, E. W.; Herrington, K. L.; Murthy, A. K. *J. Phys. Chem.* **1992**, *96*, 6698–6707.
- (48) Nettesheim, F.; Liberatore, M. W.; Hodgdon, T. K.; Wagner, N. J.; Kaler, E. W.; Vethamuthu, M. *Langmuir* **2008**, *24*, 7718–7726.
- (49) Raghavan, S. R.; Kaler, E. W. *Langmuir* **2001**, *17*, 300–306.
- (50) Kern, F.; Zana, R.; Candau, S. J. *Langmuir* **1991**, *7*, 1344–1351.
- (51) Hassan, P. A.; Manohar, C. J. *Phys. Chem. B* **1998**, *102*, 7120–7125.
- (52) Müller, A. J.; Torres, M. F.; Sáez, A. E. *Langmuir* **2004**, *20*, 3838–3841.
- (53) Gamez-Corrales, R.; Berret, J. F.; Walker, L. M.; Oberdisse, J. *Langmuir* **1999**, *15*, 6755–6763.
- (54) Kalur, G. C.; Raghavan, S. R. *J. Phys. Chem. B* **2005**, *109*, 8599–8604.
- (55) Islam, M. F.; Hough, L. A.; Alsayed, A. M.; Yodh, A. G. APS March meeting Los Angeles 2005, D37.00010.
- (56) Niyogi, S.; Boukhalfa, S.; Chikkannanavar, S. B.; McDonald, T. J.; Heben, M. J.; Doorn, S. K. *J. Am. Chem. Soc.* **2007**, *129*, 1898–1899.
- (57) Tan, Y.; Resasco, D. E. *J. Phys. Chem. B* **2005**, *109*, 14454–14460.